

A Simple Planar Antenna for Sub-6 GHz Applications in 5G Mobile Terminals

Zhirong An¹ and Mang He²

¹ School of Information and Electronics
Beijing Institute of Technology, Beijing, 100081, China
aiyindien@163.com

² School of Information and Electronics
Beijing Institute of Technology, Beijing, 100081, China
hemang@bit.edu.cn

Abstract — A simple planar antenna for sub-6 GHz applications in 5G mobile terminals is presented. The proposed antenna is composed of one multi-branch driven strip and three parasitic grounded strips, featuring simple design without using three-dimensional structure and lumped elements. The $|S_{11}| \leq -6\text{dB}$ impedance bandwidth of the antenna covers 700-960 MHz and 1600-5500 MHz bands with a compact size of $40 \times 15 \times 0.8 \text{ mm}^3$, which makes it fulfill the requirements of sub-6 GHz applications in the 5G terminals. The prototype of the antenna is fabricated, and the design is well validated by experimental results.

Index Terms — 5G terminals, multi-mode resonance, planar antenna, sub-6 GHz applications.

I. INTRODUCTION

With the rapid development of wireless communication technologies, 2G/3G/4G standard has been widely used. For current mobile terminal antennas, it is a basic requirement to cover 2G/3G/4G bands, including Long Term Evolution(LTE) 700/2300/2500 (698-787/2300-2400/2500-2690 MHz), UMTS (1920-2170 MHz), GSM 850/900 (824-894/880-960 MHz), DCS (1710-1880 MHz), and PCS (1850-1990 MHz) bands. However, to meet the recently proposed 5G NR standards, i.e., n77 (3300-4200 MHz), n78 (3300-3800 MHz), and n79 (4400-5000 MHz), such bandwidth is not enough. Therefore, it is highly desirable to design a 5G terminal antenna with wideband performance to fully cover all the 2G/3G/4G/5G bands.

Recently, several methods have been proposed to extend the bandwidth of mobile phone antennas, such as using matching networks with lumped elements [1, 2], frequency reconfigurable technique [3, 4], and multi-mode resonance technique [5, 6]. In [1], an octa-band WWAN/LTE monopole antenna with a lumped high-pass matching circuit was proposed. However, because

the matching circuit is not ideal, the resistance of the matching circuit will introduce additional losses, at the same time, it also makes the working frequency band sensitive to the value of lumped elements. In [3], a reconfigurable antenna using a PIN diode for WWAN/LTE application was also presented. PIN diode needs additional space for its DC control circuit and brings extra loss as well, which limits its practical usage. Compared with the above-mentioned two methods, multi-mode resonance technique is more convenient to fulfill the antenna optimization. In [5], a broadband antenna with multiple resonant modes was proposed for mobile handset applications, but a relatively large clearance area was needed in the design. In order to reduce the clearance area, limited designs folded the antenna into three-dimensional structures [7, 8]. Although doing so reduces the lateral size occupied by the antenna, it requires additional area in the vertical direction and at the same time it also increases the difficulty in manufacturing.

In this letter, a simple planar antenna design for sub-6 GHz applications in 5G mobile terminals is proposed. The presented antenna has a fully planar structure and no lumped elements are required, which makes it a simple structure and easy to be fabricated. Compared with other planar antenna designs, the antenna dimension provided in [5] and [6] is $68 \times 15 \text{ mm}^2$ and $60 \times 15 \text{ mm}^2$, respectively, while the antenna dimension provided in this paper is only $40 \times 15 \text{ mm}^2$, which occupies at most 67% of the clearance areas in [5] and [6] but has a wider frequency band. The measured $|S_{11}| \leq -6\text{dB}$ bandwidth covers 700-960 and 1600-5500 MHz bands, in which all the LTE 700/2300/2500, UMTS, GSM 850/900, DCS, PCS, and n77, n78, n79 bands are included.

II. ANTENNA DESIGN

As shown in Fig. 1 (a), the antenna is printed on a $135 \times 80 \times 0.8 \text{ mm}^3$ FR4 substrate with $\epsilon_r=4.4$ and $\tan\delta=$

0.02. The ground plane is a part of the bottom surface of the substrate with the size of $120 \times 80 \text{ mm}^2$. The antenna is composed of one multi-branch driven strip and three parasitic grounded strips. The driven strip has three branches as shown in Fig. 1 (b), which is printed on the top surface of the substrate and is connected to a 50Ω coaxial line at the feeding point. The parasitic grounded strips consist of three parts: the L-shaped branch and the

protrude stub are printed on the bottom surface of the substrate and are directly connected to the ground as shown in Fig. 1 (c); and the longer meandered branch shown in Fig. 1 (d) is etched on the top surface of the substrate and is connected to the ground through a via hole at the shorting point. By exhaustive parametric studies, the optimum dimensions of the antenna are listed in Table 1.

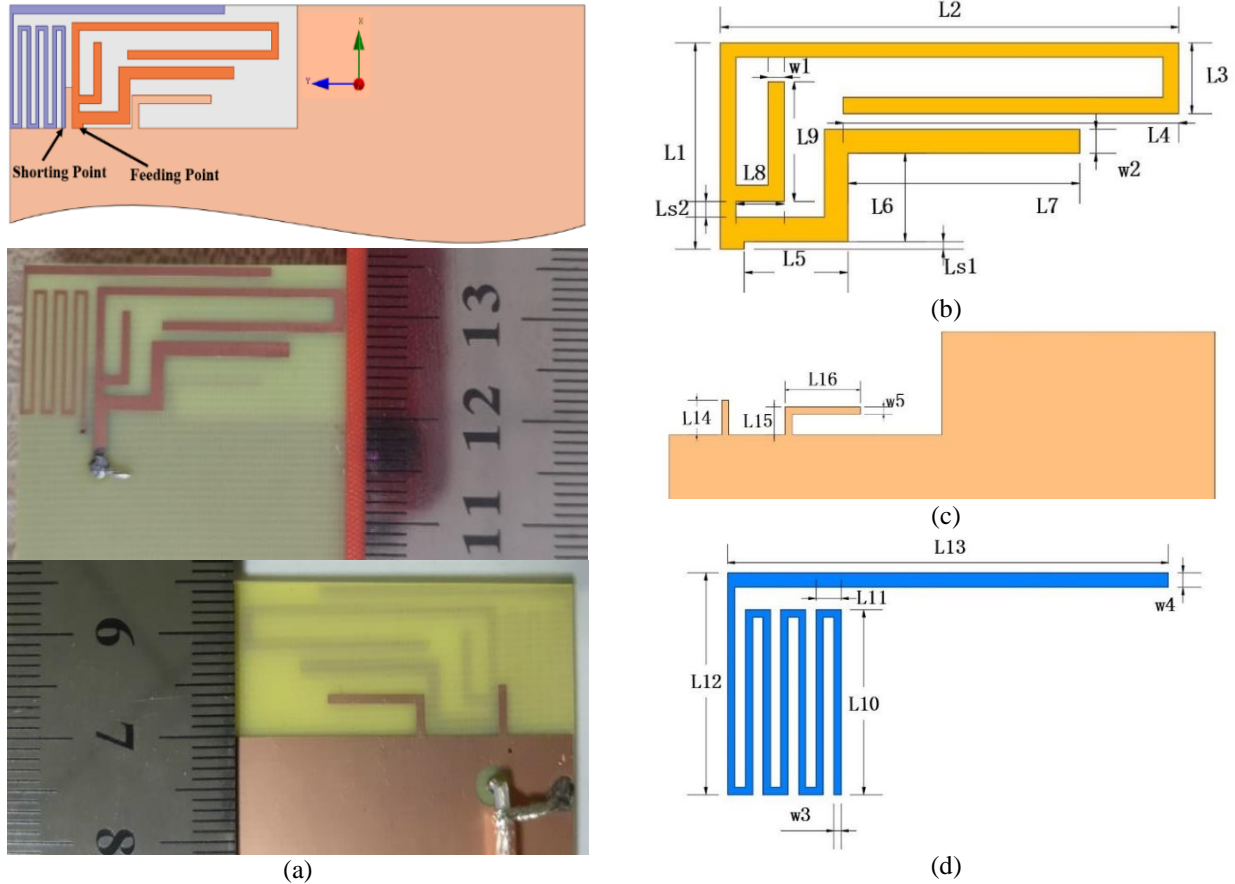


Fig. 1. Geometry of the proposed antenna: (a) antenna configuration and the fabricated prototype, (b) the driven branch, (c) the L-shaped branch and protruded stub, and (d) the meandered branch.

Table 1: Optimum dimensions of the antenna (unit: mm)

Parameters	L1	L2	L3	L4	L5	L6
Values	12.9	28.7	4.4	21	6.5	5.5
Parameters	L7	L8	L9	L10	L11	L12
Values	14.5	3	7.5	12.5	1.7	15
Parameters	L13	L14	L15	L16	w1	w2
Values	29.9	5	4	11	1	1.5
Parameters	w3	w4	w5	Ls1	Ls2	
Values	0.5	1	1	0.5	1	

III. WORKING PRINCIPLE OF THE ANTENNA

The working principle of the proposed antenna can be explained through Fig. 2. The longer branch of Ref1, we call it branch1, operates like a monopole in the $\lambda/4$ mode and generates a resonance at 0.95 GHz, and the shorter one is called branch2 and has two resonances: at 2.1 GHz the branch operates in the $\lambda/4$ mode, while at 4.7 GHz it operates in the $\lambda/2$ mode. On this basis, in order to cover the n79 band up to 5.5 GHz, it is necessary to introduce a new resonance at higher frequency. At the same time, the introduction of the new resonance should not have too much influence on the existing resonances, especially on the resonance at 4.7 GHz, in order to avoid increasing the difficulty in tuning of the antenna's structure. Therefore, the insertion position of the new branch with respect to branch1 and branch2 should be close to the feeding point, while keeping an appropriate distance from branch2. To this end, a short branch called branch3 is introduced between branch1 and branch2 as shown in Ref2. This new branch operates in its $\lambda/4$ mode and generates a new resonance at 5.3 GHz, and its effect is clearly seen in Fig. 2 (a) that the impedance bandwidth is much enhanced at high frequency end.

In addition, to include the LTE 700 and GSM 850 bands, it is necessary to generate a new resonance around 700 MHz. If a new branch is inserted into the structure of Ref2 as before, too many branches will crowd in small space, which will result in strong mutual coupling and each operating frequency of the antenna will become very difficult to control independently. Therefore, a parasitic meandered branch is introduced, which provides a $\lambda/4$ mode resonance at 0.75 GHz and at the same time two additional higher-order modes can also be generated at 2.2 GHz and 3.75 GHz, respectively.

Meanwhile, the $|S_{11}|$ versus frequency in Fig. 2 (b) indicates impedance mismatching of Ref3 from 2.7 to 3.5 GHz. To lower the reflection coefficients in this frequency range, a parasitic L-shaped branch, which is protruded from the ground on the bottom surface of the substrate and is without in touch with the driven strip, is introduced to form a new resonance around 3.35 GHz in between of 2.7 and 3.5 GHz. The parasitic branch works in the $\lambda/2$ mode at 3.35 GHz, and as shown in Fig. 2 (b) the new structure Ref4 improves reflection coefficients when compared with Ref3. However, due to the coupling between newly added L-shaped branch and branch2, impedance matching deteriorates around 4.5-5 GHz. To eliminate the mismatching, a grounded short stub is added between the meander strip and the driven branch, then the proposed antenna is formed. It can be seen from Fig. 2 that the grounded short stub improves the impedance matching of 4.5-5 GHz and the proposed antenna achieves the coverage of the required frequency band.

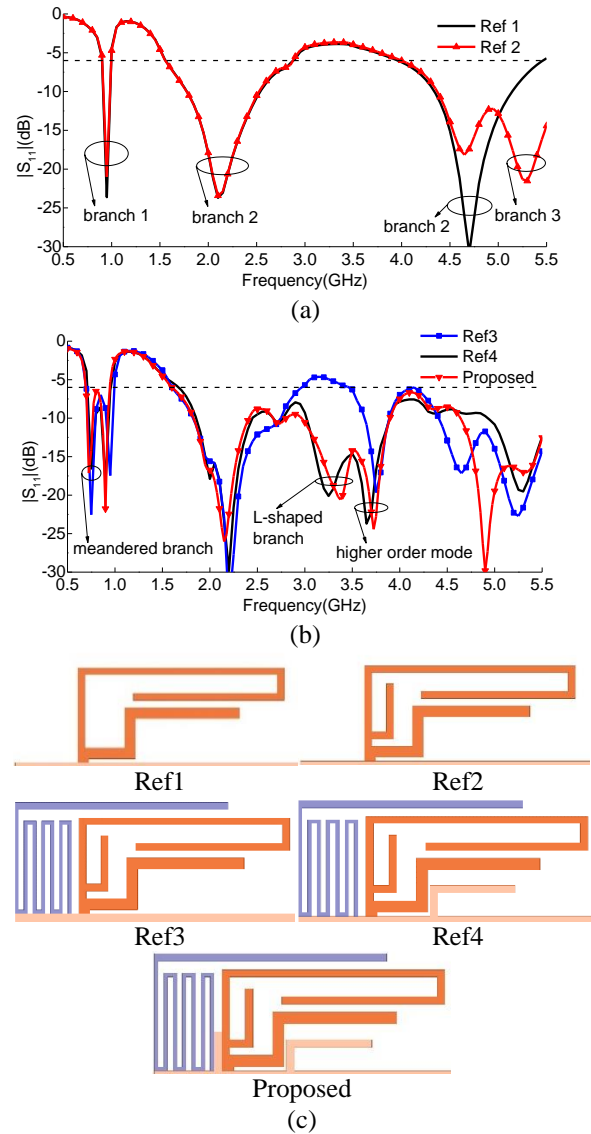


Fig. 2. Simulated $|S_{11}|$ of different antennas: (a) simulated result of Ref1 and Ref2, (b) simulated result of Ref3, Ref4 and proposed antenna, and (c) configuration of different antenna.

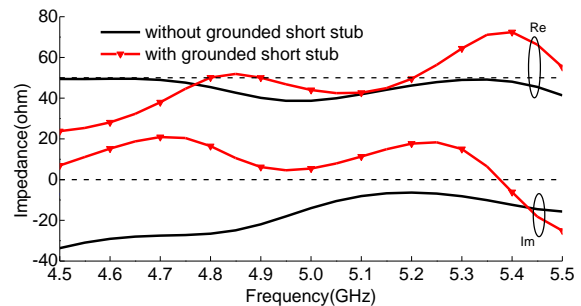


Fig. 3. Simulated impedance of different antennas.

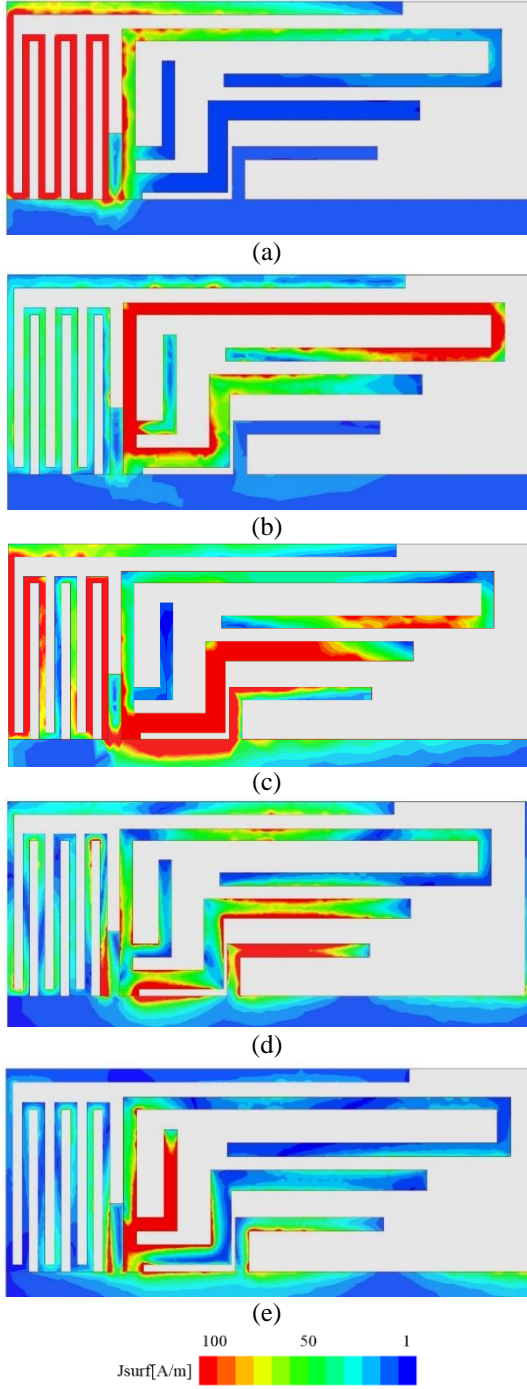


Fig. 4. Current distributions on the proposed antenna at different frequencies: (a) 0.75 GHz, (b) 0.95 GHz, (c) 2.1 GHz, (d) 3.35 GHz, and (e) 5.3 GHz.

To further understand the working principle of the grounded short stub, Fig. 3 gives the simulated impedance of Ref4 and proposed antenna. For an antenna, the definition of S_{11} is identical to the reflection

coefficient,

$$S_{11} = \Gamma. \quad (1)$$

The voltage reflection coefficient Γ is the ratio between the reflected wave and the incidence wave. Γ is defined in (2):

$$\Gamma = \frac{Z_L - Z_0}{Z_L + Z_0}, \quad (2)$$

where Z_L is the antenna impedance and Z_0 is the characteristic impedance of the transmission line, which is normally 50Ω .

As can be seen from Fig. 3, the grounded short stub acts as a shunt inductor. It changes the imaginary part of the antenna impedance to approach zero, which improves the impedance matching at 4.9 GHz resonance.

The simulated current distributions on the proposed antenna at different frequencies are shown in Fig. 4, and it can be seen that the multiple branches of the antenna generate distinct resonant modes. Meanwhile, in various operating mode, the current mainly concentrates in the corresponding branch, and the coupling between the different branches is relatively small, which is beneficial to the design and optimization of the antenna.

In Fig. 5, the simulated $|S_{11}|$ with different values of $Ls2$ which is related to the position of branch 3 is presented. It can be seen that the position of branch3 significantly affects the match at 5.3 GHz, while other existing frequencies are almost unaffected.

IV. RESULTS AND DISCUSSION

A prototype of the antenna is fabricated, and the measured $|S_{11}|$ is given in Fig. 6, which agree well with the simulated results. The difference is mainly due to the uncertainty of the dielectric constant of the FR4 substrate. For current mobile antennas, most of them are on the basis of $-6\text{dB } |S_{11}|$, which is enough for practical application [1-8]. The measured impedance bandwidth with $|S_{11}| \leq -6\text{dB}$ is over 700-960 and 1600-5500 MHz, covering all the LTE 700/2300/2500, UMTS, GSM 850/900, DCS, PCS, and n77/78/79 bands.

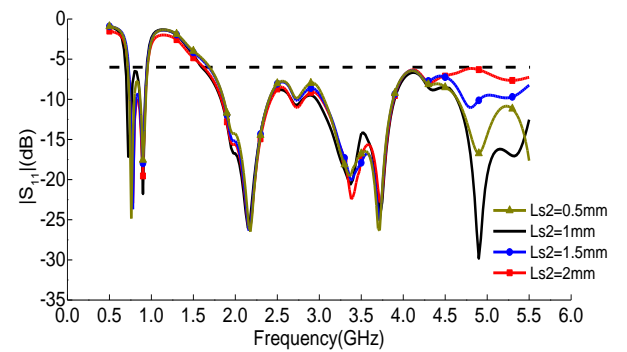


Fig. 5. Simulated $|S_{11}|$ with different values of $Ls2$.

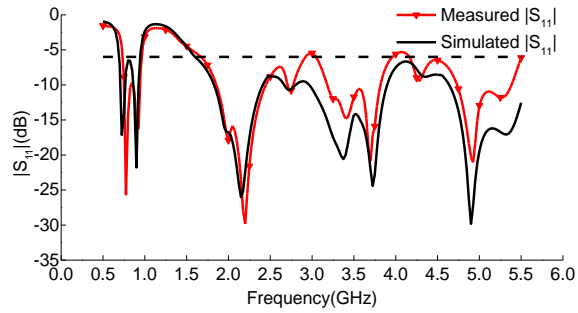


Fig. 6. Simulated and measured $|S_{11}|$ of the proposed antenna.

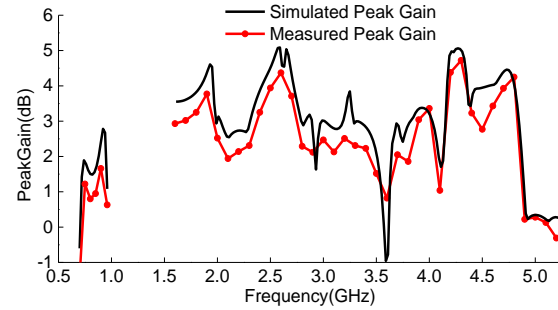


Fig. 8. Peak Gain of the proposed antenna.

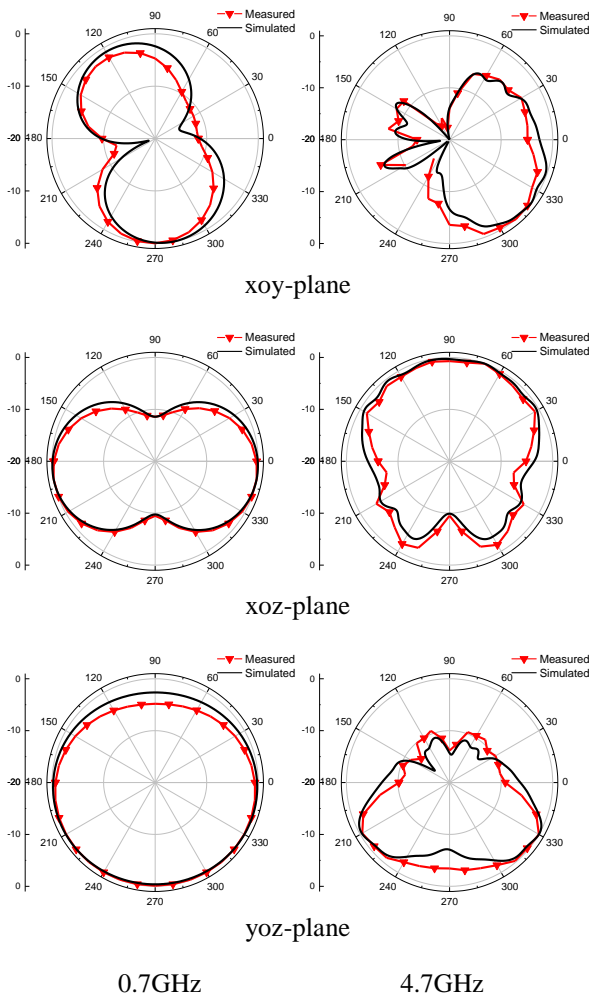


Fig. 7. Simulated and measured radiation patterns of the proposed antenna.

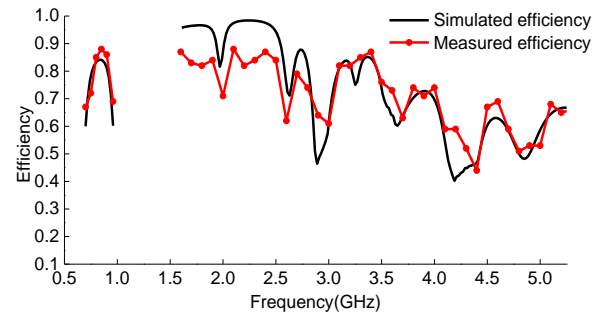


Fig. 9. Efficiency of the proposed antenna.

The simulated and measured radiation patterns at 0.7 GHz and 4.7 GHz is shown in Fig. 7. It can be observed that the antenna exhibits good monopole characteristics at 0.7 GHz, while at 4.7 GHz, since the branch2 is mainly parallel to the ground, the radiation is reflected by the ground and exhibits a unidirectional pattern. The measured and simulated peak gain are shown in Fig. 8. The measured gain ranges from -1.39 to 1.66 dBi at the low frequency band and from -1.09 to 4.72 at the high frequency band, respectively. For mobile antennas, the gain and the radiation pattern are not an important parameter, because it is mostly decided by the position in which an antenna is installed and the size of the grounding structure. The antenna element itself does not have much to do with deciding the gain and radiation patterns. In contrast, mobile antennas are more concerned with antenna efficiency. The measured efficiency is shown in Fig. 9 and agrees well with the numerical results. The efficiency is from 60% to 84% at the low frequency band and from 41% to 88% at the high frequency band, respectively. For this work, 1-1.6 GHz is not the desired operating frequency band, so the gain and efficiency of 1-1.6 GHz are not given in the figure.

Table 2: Comparison of the proposed antenna with previous works

	Operating Bands (MHz)	Dimension (mm)	Gain (dBi)	Lumped Element Using	Efficiency (%)
[1]	690-980, 1630-2740	80×8×5.8	0.3-5.6	Yes	50.2-94.5
[2]	690-1000, 1680-2950	56×5×0.8	1.3-5.2	Yes	54-83
[3]	808-965, 1696-3000	30×15×4	-2.2-3.1	Yes	28-71
[4]	698-960, 1710-2170, 2300-2690	60×10×0.8	0.5-1.45	Yes	40-84
[5]	698-1046, 1618-2703, 3018-4377, 4697-6000	68×15×0.8	0.4-5.6	No	50-87
[6]	660-1065, 1665-3000	60×15×0.8	0.5-3	No	42-88
[7]	690-970, 1680-2740	70×8×5.8	-0.06-4.02	No	51.4-86.9
[8]	670-1020, 1650-2920	80×6×5.8	1.43-4.48	No	63.2-97.2
Proposed	700-960, 1600-5500	40×15×0.8	-1.3-4.7	No	41-88

Table 2 shows performance comparison of the proposed antenna with previous works. Unlike the designs in [1-4], no lumped elements are required in the present design, which reduces the difficulty in antenna manufacturing. As well, it can be seen that the proposed antenna occupies at most 67% space to achieve comparable or even wider bandwidth as compared with the works presented in [5-6]. Actually, the fabrication of the antenna is even easier than those in [7] and [8], since the antenna is a fully planar structure and no vertical space is needed. Therefore, the proposed antenna has advantages of wide bandwidth, small size, and easy manufacturability, which makes it suitable for sub-6 GHz applications in 5G mobile terminals.

V. CONCLUSION

A simple wideband planar antenna for sub-6 GHz applications in 5G mobile terminals is presented. The antenna covers the desired frequency band by exciting multiple operating modes. The design process and working mechanism are described and analyzed in detail, and the measured results are in good agreement with the simulated ones. Low profile, wide bandwidth, and no need of lumped-element loadings makes this design has a good application value.

REFERENCES

- [1] Y. Wang and Z. Du, "Wideband monopole antenna with less nonground portion for octa-band WWAN/LTE mobile phones," *IEEE Trans. Antennas Propag.*, vol. 64, no. 1, pp. 383-388, Jan. 2016.
- [2] Y. Liu, Y. Luo, and S. Gong, "An antenna with a stair-like ground branch for octa-band narrow-frame mobile phone," *IEEE Antennas Wireless Propag. Lett.*, vol. 17, no. 8, pp. 1542-1546, Aug. 2018.
- [3] Y. Xu, Y. Liang, and H. Zhou, "Small-size reconfigurable antenna for WWAN/LTE/GNSS smartphone applications," *IET Microw., Antennas Propag.*, vol. 11, no. 6, pp. 923-928, 2017.
- [4] Y. Liu, P. Liu, Z. Meng, L. Wang, and Y. Li, "A planar printed nona-band loop-monopole reconfigurable antenna for mobile handsets," *IEEE Antennas Wireless Propag. Lett.*, vol. 17, no. 8, pp. 1575-1579, Aug. 2018.
- [5] X. Wang, Y. Wu, W. Wang, and A. A. Kishk, "A simple multi-broadband planar antenna for LTE/GSM/UMTS and WLAN/WiMAX mobile handset applications," *IEEE Access*, vol. 6, pp. 74453-74461, 2018.
- [6] C. Deng, Y. Li, Z. Zhang, and Z. Feng, "Planar printed multi-resonant antenna for octa-band WWAN/LTE mobile handset," *IEEE Antennas Wireless Propag. Lett.*, vol. 14, pp. 1734-1737, 2015.
- [7] R. Tang and Z. Du, "Wideband monopole without lumped elements for octa-band narrow-frame LTE smartphone," *IEEE Antennas Wireless Propag. Lett.*, vol. 16, pp. 720-723, 2017.
- [8] D. Huang, Z. Du, and Y. Wang, "An octa-band monopole antenna with a small nonground portion height for LTE/WLAN mobile phones," *IEEE Trans. Antennas Propag.*, vol. 65, no. 2, pp. 878-882, Feb. 2017.